

# A Practical Approach for Exploration and Modeling of the Design Space of a Bacterial Vaccine Cultivation Process

M. Streefland,<sup>1</sup> P.F.G. Van Herpen,<sup>1</sup> B. Van de Waterbeemd,<sup>1</sup> L.A. Van der Pol,<sup>1</sup>  
E.C. Beuvery,<sup>2</sup> J. Tramper,<sup>3</sup> D.E. Martens,<sup>3</sup> M. Toft<sup>4</sup>

<sup>1</sup>Netherlands Vaccine Institute, Unit Research and Development,  
PO Box 457, 3720 AL Bilthoven, The Netherlands; telephone: 31-30-274-2066;  
Fax: 31-30-274-4426; e-mail: mathieu.streefland@nvi-vaccin.nl

<sup>2</sup>PAT Consultancy, Vianen, The Netherlands

<sup>3</sup>Department Bioprocess Engineering, Wageningen University, EV Wageningen,  
The Netherlands

<sup>4</sup>Umetrics AB, Malmö, Sweden

Received 18 February 2009; revision received 14 May 2009; accepted 22 May 2009

Published online 1 June 2009 in Wiley InterScience (www.interscience.wiley.com). DOI 10.1002/bit.22425

**ABSTRACT:** A licensed pharmaceutical process is required to be executed within the validated ranges throughout the lifetime of product manufacturing. Changes to the process, especially for processes involving biological products, usually require the manufacturer to demonstrate that the safety and efficacy of the product remains unchanged by new or additional clinical testing. Recent changes in the regulations for pharmaceutical processing allow broader ranges of process settings to be submitted for regulatory approval, the so-called process design space, which means that a manufacturer can optimize his process within the submitted ranges after the product has entered the market, which allows flexible processes. In this article, the applicability of this concept of the process design space is investigated for the cultivation process step for a vaccine against whooping cough disease. An experimental design (DoE) is applied to investigate the ranges of critical process parameters that still result in a product that meets specifications. The on-line process data, including near infrared spectroscopy, are used to build a descriptive model of the processes used in the experimental design. Finally, the data of all processes are integrated in a multivariate batch monitoring model that represents the investigated process design space. This article demonstrates how the general principles of PAT and process design space can be applied for an undefined biological product such as a whole cell vaccine. The approach chosen for model development described here, allows on line monitoring and control of cultivation batches in order to assure in real time that a process is running within the process design space.

Biotechnol. Bioeng. 2009;104: 492–504.

© 2009 Wiley Periodicals, Inc.

**KEYWORDS:** process analytical technology; PAT; *Bordetella pertussis*; process design space; process model; cultivation; DoE

## Introduction

“The process design space is the multidimensional combination and interaction of input variables (e.g., material attributes) and process parameters that have been demonstrated to provide assurance of quality” (ICH, 2005). This is the definition of process design space proposed by ICH, the International Conference for the Harmonization of Pharmaceutical Regulation. The word *design* indicates the requirement for a rationale behind process development. The design of a process that can consistently assure the yield of products with the desired quality is one of the key elements of the Process Analytical Technology (PAT) initiative introduced by the American Food and Drug Administration (FDA) in 2004 (FDA, 2004). The FDA defines PAT as a “system for designing, analyzing and controlling manufacturing through timely measurements of critical quality and performance attributes of raw and in-process materials and processes, with the goal of ensuring final product quality.”

The development and use of a design space is concisely described in the Annex to the ICH Q8 Guideline on Pharmaceutical Development (ICH, 2005). Originally, the concept of PAT and design space applied only to chemical

Correspondence to: M. Streefland

drugs. However, the principles behind PAT and of the design space can be readily extended to biopharmaceuticals as is demonstrated in this article and reported earlier by others (Harms et al., 2008).

Prior to the introduction of the design space concept, process validation relied initially on the execution of three consecutive conformity batches that demonstrated process robustness.

The design space concept allows manufacturers to move away from fixed processes, permitting process variation after sufficient understanding and control of the process and knowledge of the impact of process variation on product performance have been demonstrated. In such a case, a change of the process settings or trajectory within an approved design space is not considered a deviation in the regulatory sense of the word (i.e., it does not require regulatory approval).

One way of demonstrating the understanding of the process and its variation is to investigate the critical process parameters using Design of Experiments or DoE (Montgomery, 2001). DoE investigates not only the impact of the variation of a single, critical parameter, but also any interactions that these critical parameters might have with each other. For instance, a process might be running fine at high temperature or low pH, but the combination of these two process conditions could be unfavorable for product quality.

The mapping of a process begins with an understanding of the critical product quality attributes, for example, in the case of vaccines, the antigens that induce the protective immune response. The next step is the identification of those process parameters that influence process performance (e.g., yield) or the critical product quality attributes (e.g., antigen expression). These parameters can be anything from the quality of (complex) starting materials (such as bovine serum or yeast extract) to the pH and temperature during processing.

Once the critical process and product attributes are known, the failure limits of the process can be investigated. These are the limits of critical process parameters at which the critical product quality attributes are so compromised that the product will no longer meet its specifications or that the process will fail altogether. With existing products, some specific limits are well known to the operators that run the process routinely, while others are generally known to be common for a broad range of processes. For instance the upper temperature limit of a cultivation process step can usually not exceed 40°C for most organisms, because cellular processes are radically changed or even disrupted at high temperatures. The failure limits or critical limits for any remaining parameters can be investigated with a series of simple experiments, such as we reported for dissolved oxygen concentration (Streetland et al., 2008).

The combination of the failure limits does not, by itself, constitute a design space since it provides no means for predictions outside of the actually tested settings. Rather, the knowledge gained from the evaluation of failure limits can

be used to devise a DoE experimental matrix to determine the design space. The results from a DoE experimental matrix can be modeled so that predictions can be made for a continuous range of settings and their interactions, based on a discrete number of tested settings. Test values for the critical process parameters that are known to yield product of specified quality within the process failure limits are selected for the matrix. The tested ranges of the critical parameters then provide the boundaries of a multidimensional space having the number of its dimensions equal to the number of critical parameters in the design.

Biopharmaceutical products are typically produced in a batch-wise manner, and this gives rise to three-way data arrays: batch number versus processing time versus process parameters (see also Fig. 2). Chemometric methods such as principal component analysis (PCA) and partial least squares (PLS) calibration models (Wold et al., 2008) can be used to model the three-way batch data in order to provide tools for understanding, fault detection, control, and prediction. The resulting dynamic control models can be used to describe a (partial) design space, taking into account the evolution of parameters during processing.

In this article, we investigate the design space for the cultivation of *Bordetella pertussis* bacteria. This is the key process step in the manufacturing of a whole cell vaccine against whooping cough disease. A whole cell vaccine means that the whole bacterial cell is the actual product, in contrast to, for instance, sub unit vaccines in which only purified membrane proteins are used. The downstream processing of such a vaccine involves only inactivation and concentration of the cells without a purification step. Thus, the most critical product quality characteristics are already defined at the end of the cultivation process.

In order to *consistently ensure a predefined quality at the end of the manufacturing process* (ICH definition of the scope

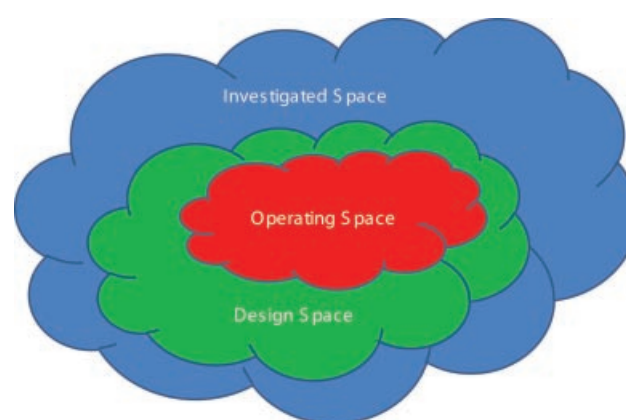


**Figure 1.** The Design Space as a sub-space of the Investigated Space (also known as the Knowledge Space). The Operating Space (where the process is intended to run) can be a large or small part of the Design Space (adapted from Harms et al., 2008). [Color figure can be seen in the online version of this article, available at [www.interscience.wiley.com](http://www.interscience.wiley.com).]

of PAT), an additional signal may be needed that can be related to process performance or product quality. According to the FDA's PAT guidance, "Measurements collected from these process analyzers need not be absolute values of the attribute of interest." In this study, near infrared (NIR) spectroscopy is investigated as a PAT tool, that is, *an online measurement of critical quality and performance attributes* (FDA/ICH PAT definition), to monitor the cultivation of *B. pertussis* bacteria. NIR data are used to indicate specific attributes of interest (such as biomass concentration) and as a "fingerprint" that gives qualitative information on the status and trajectory of the process. All data gathered online—NIR as well as conventional cultivation process data (i.e., pH, temperature, and gasflow controller outputs)—are combined in a single database using PAT compliant software. This database contains all data used to construct the model describing the multivariate process design space.

The design, experimentation and multivariate modeling required to define the design space for the cultivation of *B. pertussis* are described. The resulting process model integrates bioreactor control data with online NIR measurements and can be used for on-line, real time modeling of the cultivation process. This provides real time assurance of process performance and an indication of product quality during processing. Ultimately, the system will be capable of real time release of the cultivation product for further processing.

The main goal of this article is to investigate the applicability of the principles of design space investigation for a complex biopharmaceutical cultivation process. We investigate both the experimental work involved, the analytical (PAT) tools used and the data processing and modeling necessary in order to devise a model that describes the process design space. It is a first attempt to apply the principals of PAT and process design space for an undefined biopharmaceutical product, namely a whole cell vaccine. While the manufacturing process is relatively simple, the product itself can be regarded as the "worst case" in terms of how defined and how well characterized the product is. The ability to apply PAT principles on this product bodes well

for the implementation of PAT on other, more defined (bio)pharmaceutical products.

## Materials and Methods

### Experimental Design

An experimental design was executed and data from the design used to mathematically model the effects of the process parameters on product quality. A robustness design in which the parameter values chosen were at a safe margin from known or expected failure limits was employed. The design was a Plackett Burman design in 8 runs to which two times two replicate center points were added (two for each of the two reactors). The experimental matrix, having 12 runs, is shown in Table I. Experiment 6 was done twice, owing to a data collection problem, once in Reactor A and once in Reactor B.

The process parameters investigated were: the dissolved oxygen (DO), the pH, the temperature, the density of bacteria at the end of the pre-culture phase in the shake-flask (Preculture density), the actual density of bacteria at the start of the bioreactor run (Inoculation density), and which of the two identical bioreactor systems, A or B, was used in the experiment.

### Bioreactor Cultivations

#### Cultivation Conditions

All cultivations were carried out in a fully instrumented 7 L *in situ*, sterilizable bench-top bioreactor with a six-bladed Rushton turbine (Applikon, Schiedam, The Netherlands). The bioreactor was filled with 4 L of THIJS medium (Thalen et al., 1999) and raised to the set point temperature and a 100% dissolved oxygen (DO) condition. It was then inoculated with preculture from a shake-flask at an optical density at 590 nm ( $OD_{590}$ ) of 0.5, 1.0, or 1.5. The volume of preculture used to inoculate the bioreactors was adjusted to

**Table I.** The DoE matrix for the 12 batch runs used to determine the process design space.

Experiment number	Run order	DO (%)	pH	Temperature (°C)	Preculture density	Inoculation density	Reactor
1	1	10	6.8	37	0.5	0.1	A
2	12	60	6.8	33	0.5	0.025	B
3	2	60	6.8	37	1.5	0.025	A
4	3	30	7.2	35	1	0.05	B
5	4	30	7.2	35	1	0.05	A
6B	10	10	7.8	37	0.5	0.025	B
6A	13	10	7.8	37	0.5	0.025	A
7	5	60	7.8	33	0.5	0.1	A
8	6	30	7.2	35	1	0.05	B
9	7	10	7.8	33	1.5	0.025	A
10	8	60	7.8	37	1.5	0.1	B
11	11	30	7.2	35	1	0.05	A
12	9	10	6.8	33	1.5	0.1	B

yield the desired starting density. Temperature, DO, pH and stirrer speed were controlled at the different values shown in Table I. A low-drift polarographic electrode (Applikon) was used to measure the dissolved oxygen concentration in the liquid (DO). pH and temperature were measured using a glass pH electrode (Mettler Toledo, Tiel, The Netherlands) and a Pt100 temperature sensor (Applikon), respectively. All sensors were connected to the bioreactor control system (Applikon), which was operated using PCS7-based bioreactor control software (Siemens, Zwijndrecht, Belgium). DO was controlled with increments in stirrer speed up to 650 rpm after which it was controlled by increasing the fraction of oxygen in the headspace. The fraction of air, O<sub>2</sub>, and N<sub>2</sub> were also registered in the control system. Total gas flow was kept constant at 1.0 L/min.

### Nutrient Concentration Analysis

Samples were taken at regular intervals and OD<sub>590</sub> and nutrient concentrations were measured. Samples were sterile filtered (0.22 µm) and supernatants were stored at -20°C for further nutrient analysis. Lactate and glutamate concentrations were determined by <sup>1</sup>H-nuclear magnetic resonance (NMR) spectroscopy using a JEOL JNM ECP 400 spectrometer operating at 400MHz (JEOL, Tokyo, Japan) and equipped with a JEOL Stacman autosampler for 16 samples. Supernatants were analyzed by adding 0.1 mL of D<sub>2</sub>O containing 3-(trimethylsilyl)[D4]propionic acid sodium salt (TSP, 0.167 mM) to a 0.9 mL sample. The water signal was suppressed by a standard pulse experiment using presaturation. The spectra were referenced using the TSP signal at 0 ppm. Lactate and glutamate concentrations were quantified by integration of the relevant signals. NMR was also used to check samples for any waste metabolites.

### Data Collection and Handling

All on line data necessary to build the process model were collected using the SIPAT software. Every 2 min this software collected the data from the cultivation system and the NIR system (see below) and stored it in a central database. When two bioreactor systems were running simultaneously, the SIPAT software collected the data from each system sequentially every minute so that each system was still sampled every 2 min. The SIPAT database was later used to build the process model.

### NIR Spectroscopy Measurements

An on-line NIR transmission probe (Solvias AG, Basel, Switzerland) with a fixed path length of 5 mm, was implemented in both bioreactor vessels. The probe was immersed in the liquid with the measurement slit at the height of the stirrer, pointing away from the stirrer. Measurements were made every 2 min on both probes using a Bruker Matrix F NIR source (Bruker Optics, Ettlingen, Germany). Spectra were taken at a resolution of 4 cm<sup>-1</sup>

between 12,000 and 4,000 cm<sup>-1</sup>. Each spectrum was an average of 32 scans.

### Additional Samples for PLS Calibration of Biomass Density

Some additional samples were necessary to build a suitable PLS calibration model for biomass density. The samples were prepared by cultivating *B. pertussis* in a glass shake-flask according to the standard procedure. At the end of the cultivation (OD = 1.3–1.5), half of the shake-flask was centrifuged and sterile filtered to yield cell-free supernatant. Suspension and cell-free supernatant were mixed to create samples with optical densities that match, the start, half-time and end of the cultivation, but that have nutrient concentrations that do not match these cultivation stages. In this way, the correlation between optical density and nutrient concentration is disconnected, in order to see if these parameters individually correlate to the NIR signal and that they not merely have the same process trend Table II.

Lactate and glutamate stock solutions were prepared at 4.44 and 2.22 M, respectively. These solution were mixed according to a full factorial design to produce concentrations typical for the start, halftime or end of a standard cultivation. Half-time samples were prepared by mixing cell-free supernatant with cell suspension at a dilution of 1:1. The cell-free supernatant was used as a surrogate for the low-OD samples.

In total, 27 were samples were prepared and, after thorough mixing, were quickly measured using an NIR cuvette bench (Bruker Optics, Ettlingen, Germany). The settings were identical to those used for the transmission probe inside the bioreactor.

### Microarray Analysis

#### RNA Isolation

Samples for microarray analysis were taken at the end of each cultivation. For fixation of the RNA expression profile,

**Table II.** DoE experiments and their corresponding product quality scores.

Experiment number	Product quality score
01	10.36
02	10.00
03	9.95
04	8.89
05	9.68
06B	9.74
06A	8.57
07	9.67
08	10.07
09	9.51
10	9.91
11	10.58
12	10.53

one volume of bacterial culture was mixed with two volumes of *RNase retarding solution* (Kasahara et al., 2006; Mutter et al., 2004; Ramalho et al., 2004). For each microarray sample 2.5 mL cultivation at  $OD_{590} = 1.0$  was used. Samples at other optical densities were adjusted accordingly, so that an equal amount of cells was used for each sample. The samples were concentrated by centrifugation and treated for 3 min with Tris-EDTA buffer, containing 0.5 mg/mL lysozyme (Sigma-Aldrich, Zwijndrecht, The Netherlands). Total RNA was extracted with the SV total RNA isolation system (Promega Benelux, Leiden, The Netherlands) according to the manufacturer's protocol. Nucleic acid concentration was adjusted by precipitation. UV spectral analysis was used to determine final nucleic acid concentration and purity and RNA integrity was confirmed with the Bioanalyzer RNA6000 Nano assay (Agilent Technologies, Amstelveen, The Netherlands), according to the manufacturer's protocol.

#### cDNA Labeling and Hybridization Reactions

Total RNA from all experimental samples was reverse transcribed to cDNA and labeled with Cy3/Cy5 dyes using the Chipshot Indirect Labeling Kit (Promega Benelux) according to manufacturer's protocol, with one deviation: 2  $\mu$ L random nonamer primer and no oligo-dT primer was used per reaction to reverse transcribe the total RNA, because prokaryote mRNA does not have poly-A tails. Experimental samples (Cy5) were pooled with a common reference sample (Cy3) having equal amounts of RNA from all experimental samples in the experiment. Volumes of the combined cDNA samples were adjusted to 25  $\mu$ L and an equal amount of hybridization buffer was added, to a final concentration of 25% formamide, 5 $\times$  SSC and 0.1% SDS. Samples were applied to the microarray slides and placed in a hybridization chamber (GeneMachines, San Carlos, CA) for 16–20 h at 42°C in the dark.

The microarrays were scanned with a ScanArray Express microarray scanner (Perkin Elmer, Groningen,

The Netherlands) and median fluorescence intensities were quantified for each spot using ArrayVision software (Imaging Research, Roosendaal, The Netherlands).

#### Processing of the Expression Data

The expression data were natural-log transformed, quantile normalized, corrected for the common reference dye signal and the values of replicate spots were averaged. These data processing steps were carried out using the free statistical software R, running an in-house developed script.

A product quality score was calculated from the gene expression data as described earlier (Van de Waterbeemd et al., 2009). To calculate the product quality score, only genes from the *virulence core regulon* (Cummings et al., 2006; Streefstra et al., 2007) were considered, since these are the genes that are considered to be critical for the function of the vaccine. Based on earlier work, a product quality score of 8 or higher, can be considered to represent good quality (Van de Waterbeemd et al., 2009).

#### Data Analysis and Modeling

The data available in this study can be categorized as follows (Fig. 2):

- $X_{DoE}$ : the setup parameters from the DoE (T, pH, DO, preculture density, inoculation density and reactor).
- $X_{proc}$ : the time varying process variables measured throughout the batch evolution (pH, DO, T, flow of air, O<sub>2</sub>, and N<sub>2</sub>, stirrer speed).
- $X_{NIR}$ : the on-line NIR data measured throughout the batch evolution.
- $Y_{procQ}$ : the process variables related to process evolution measured at-line by taking out samples during the cultivation (OD, glutamate and lactate).
- $Y_{prodQ}$ : the final product quality variables measured after the completion of the batch, that is, the microarray

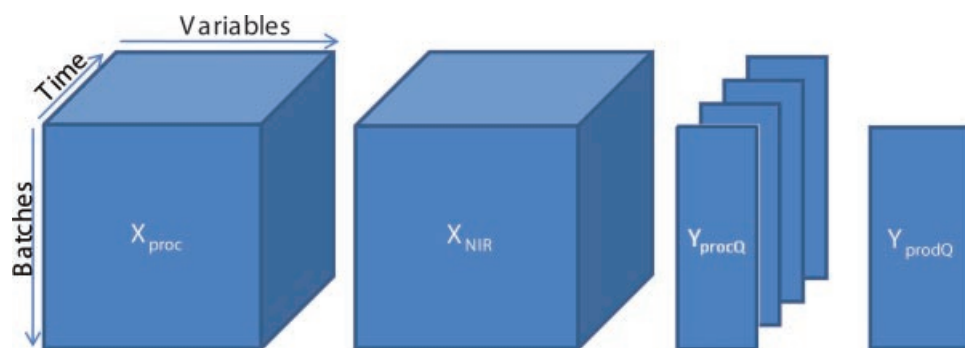


**Figure 2.** Overview of available data blocks. [Color figure can be seen in the online version of this article, available at [www.interscience.wiley.com](http://www.interscience.wiley.com).]

expression data (product quality score, see Microarray Analysis Section).

Due to the large number of distinct data sets available for the study, the analysis was split up into four sub-steps.

### *Step 1: Traditional Design Space Analysis*

The gene expression data ( $Y_{\text{prodQ}}$ ) were transformed into a product quality score and the relationship between the design setup parameters ( $X_{\text{DoE}}$ , Table I) and the product quality score was modeled to detect significant effects. The approach involved a traditional DoE analysis in which the output of the experiments was associated with the input settings. Multiple linear regression (MLR) was used to model the relationship between the process parameters and the product quality using the MODDE (Umetrics AB, Malmö, Sweden) DoE software package. A robust design space should result in a non-significant model in which no significant relationship exists between product quality and variation in the process setting within the tested range. In that case the process is stable within the design space.

### *Step 2: Prediction of Process Variables From NIR Data*

The process evolution variables ( $Y_{\text{procQ}}$ ) OD<sub>590</sub>, lactate and glutamate are a measure of the status of the cultivation and can be used to assess changes in specific growth rate or metabolism. However, these parameters are only measured at distinct sample points during cultivation. It is of interest to have these variables available on line for more accurate monitoring of the status of the cultivation. NIR data were used in an attempt to predict these process evolution variables. NIR data values were used as an  $X$  data matrix with the process evolution variables as the  $Y$  data matrix. A PLS regression model was fitted to the two datasets. The NIR data were centered before fitting the PLS model, while the process evolution data were centered and scaled to unit variance.

Initial modeling revealed a high degree of correlation between the three process evolution variables, OD<sub>590</sub>, lactate and glutamate. Therefore, a prediction model based only on the samples taken from the cultivations was not reliable. Additional samples having the three evolution variables uncorrelated with each other were therefore prepared as described in Table II earlier. These samples were also subjected to NIR spectroscopy analysis and the data were added to that from the cultivations to obtain a reliable prediction model.

### *Step 3: PCA Fingerprints From NIR Data*

The NIR measurement results in more than 4,000 variables, which are not mathematically independent and which do not all carry unique information. To use NIR data as a

“fingerprint” of the status of the process, the spectra are compressed into a small number of independent Principal Components that summarize the variation in the large number of initial variables. The computational time needed for the calculation was reduced by using one spectrum per hour for the calculation of the PCA model for each batch. Finally, all spectra (taken every 2 min) were compressed using this model.

The “fingerprint” derived from the NIR spectra does not necessarily represent specific physical or chemical characteristics of the samples, but may contain more abstract characteristics. It is assumed, however, that the NIR fingerprints are similar for all batches, thus that it can be used as a non-specific variable for the monitoring of batch evolution, allowing non-biased batch-to-batch comparisons.

### *Step 4: Building the Process Control Model*

The process data registered during batch evolution (denoted  $X_{\text{proc}}$  in Fig. 2) were modeled together with the OD<sub>590</sub> predicted from NIR (Step 2) and the NIR fingerprint variables (Step 3). Together they constitute a three-dimensional data matrix of batches versus variables (process variables, predicted OD<sub>590</sub> data, and NIR fingerprint variables) versus process time.

The evolution was split up into two phases for each batch. The first phase was represented by the part of the cultivation in which Dissolved Oxygen concentration (DO) was controlled by increments in stirrer speed and the second in which DO was controlled by increasing the fraction of O<sub>2</sub> in the headspace. This was done to allow for a different correlation structure in the process variables before and after the change in DO control strategy.

The data were modeled as described in Wold et al. (2008) using the modeling setup denoted Observation-Wise Unfolding with subsequent Batch-Wise Unfolding of the scores (OWU-BWU).

## **Software**

ArrayVision 8.0 (GE Healthcare, Uppsala, Sweden) was used to quantify microarray fluorescence intensities.

R (WU Wien, Austria) was used for statistical analysis of gene expression data.

MODDE (Umetrics, Umeå, Sweden) version 8 was used for setting up the design and for the traditional DoE analysis.

SIMCA-P+ version 11.5 (Umetrics, Umeå, Sweden) was used for all NIR data analysis as well as for building the process control model.

The SIPAT software (Siemens, Nynove, Belgium) was used for collecting process and NIR data during the cultivations and served as the database for extracting data for use in the NIR and process models.

## Results and Discussion

### Traditional Design Space Analysis

The product quality at the end of each of the 13 runs was determined by calculating the product quality score for each batch (Van de Waterbeemd et al., 2009) from the gene expression data (Table II). Prior experimentation showed that good quality is represented by a score above 8 (Van de Waterbeemd et al., 2009), and thus the scores in Table II (all higher than 8.5) should represent good product quality.

The quality scores are used instead of the actual animal (Kendrick) tests for product quality that are normally required by the authorities for whooping cough vaccine. This test involves an intra-cranial challenge of mice previously vaccinated with a human dose of vaccine with live *B. pertussis* bacteria (Irwin and Standfast, 1957; Kendrick et al., 1947). This test is not only highly variable and very cruel to the animals, but also costly and labor intensive (Xing et al., 2001). The product quality scores are therefore better suited for building this preliminary process model.

Using the DoE setup parameters as input ( $X$ ) variables and the product quality scores as output ( $Y$ ) variables, a traditional DoE analysis was done using MODDE software. No significant model could be fitted (best fit:  $R^2 = 0.38$ ;  $Q^2 = -0.2$ ), indicating that, within the ranges of the variables of the DoE setup, variation in the value of the input parameters had no effect on the product quality. This indicates that, within the tested ranges, the process is robust. The ranges tested in this study can therefore qualify as a design space as intended in the ICH Q8 Guideline (ICH,

2005). The data collected during these experiments can be used to fit a model that describes the process and can later be used as an on-line check of whether a new process is running within the design space.

### Prediction of Process Variables From NIR Data

A raw data plot of the NIR data is shown in Figure 3. The plot shows clear offset differences between the spectra, probably due to difference in optical density of the samples. No attempt was made to remove this variation as this parameter is probably the main correlate for optical density in the NIR signal, which is one of the process evolution variables to be predicted from the NIR spectra.

The very strong signals from water in the spectral regions 7,200–6,500 and 5,400–4,000  $\text{cm}^{-1}$  saturated the detector and, therefore, models built on the NIR spectra exclude these regions. The main benefit of this method is that the signal outside the “water region” is much stronger which increases the sensitivity of the measurement.

A PLS model was built from the NIR spectra ( $X$ ) and all three processes evolution variables: OD<sub>590</sub>, lactate and glutamate ( $Y$ ). This model provided very good results with a cross-validated explained variance ( $Q_Y^2$ ) of 81–97% for the three parameters. However, the three parameters were highly correlated, because OD is initially low in a cultivation, while the concentration of nutrients is high. As the cultivation proceeds, the OD increases while concentration of nutrients decrease at the same rate. Thus predictions from this model cannot be trusted, because the model is unable to predict samples correctly where this relationship between the three variables is not present. Artificial samples were

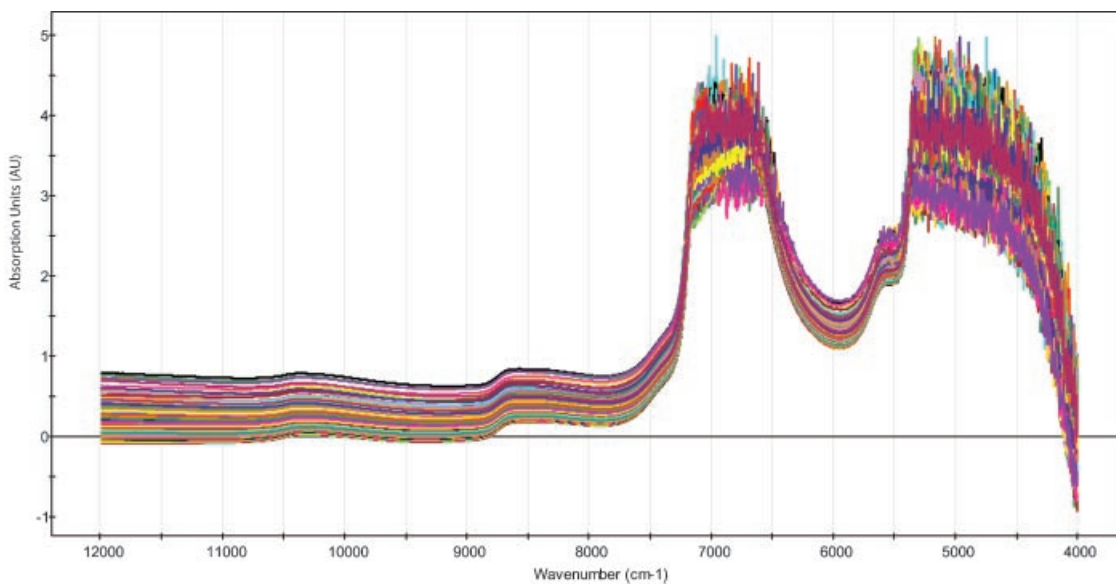


**Figure 3.** Raw data plot of NIR spectra of the samples taken out during cultivation. [Color figure can be seen in the online version of this article, available at [www.interscience.wiley.com](http://www.interscience.wiley.com).]

prepared in order to break up the correlation between the three process evolution variables. PLS models built only on these samples showed that OD could be reasonably predicted, while no significant components were found for the prediction models for lactate and glutamate.

To incorporate any difference between the spectra for the artificial samples prepared from a shake-flask cultivation and the samples taken directly from the bioreactor cultivations, a PLS model for predicting  $OD_{590}$  that was based on both sets of samples was built (total samples number: 85 (58 original cultivation samples and 27 additional samples)). The model showed very good predictive ability ( $Q^2_Y$  was 96%) and no difference between prediction error of the artificial samples and the original cultivation samples was seen (Fig. 4). The predicted values of  $OD_{590}$  were used in the subsequent analysis of batch evolution together with the process variables. This prediction model, based on the NIR signal, can be executed during cultivation of future batches, allowing a growth curve to be plotted in real time without the need for excessive sampling. However, the prediction of the higher values  $OD_{590}$  still show a large prediction error, which means that more samples from more batches need to be added to the model in order to increase its reliability before it can replace manual sampling completely.

### PCA Fingerprints From NIR Data

NIR data can also serve as a fingerprint of the status of the process. For this purpose, a Principal Component Analysis

(PCA) based model was created from the NIR cultivations data. To reduce calculation time, one spectrum per hour was used to construct the model (incorporating the entire biological evolution of the batches), resulting in a total of 218 NIR spectra. The regions containing the water signals were excluded as described above.

A PCA model with five components was created that explained 99.9% of the variation in the data. All NIR spectra (acquired every 2 min throughout the cultivations) were then compressed into these five components using this model. The five components, used as five fingerprint variables (NIR\_fp1 to NIR\_fp5), together with the process variables are used in the subsequent analysis of batch evolution.

### Building the Process Control Model

#### Integrity of Process Data

Due to an overnight data collection error, the middle part of the process and NIR data for Batches 3 and 6B were lost (~30–40% of total batch data), which means these data could not be used in the model. The data from samples taken from these batches were used, however. Process and NIR data for Batches 2, 8, 10, 11, and 12 were not sampled consistently every 2 min throughout batch evolution due to a wrong setting of the NIR sampling method. The interval for these batches varied generally between 1 and 5 min, which is adequate for batch modeling, so the batches could

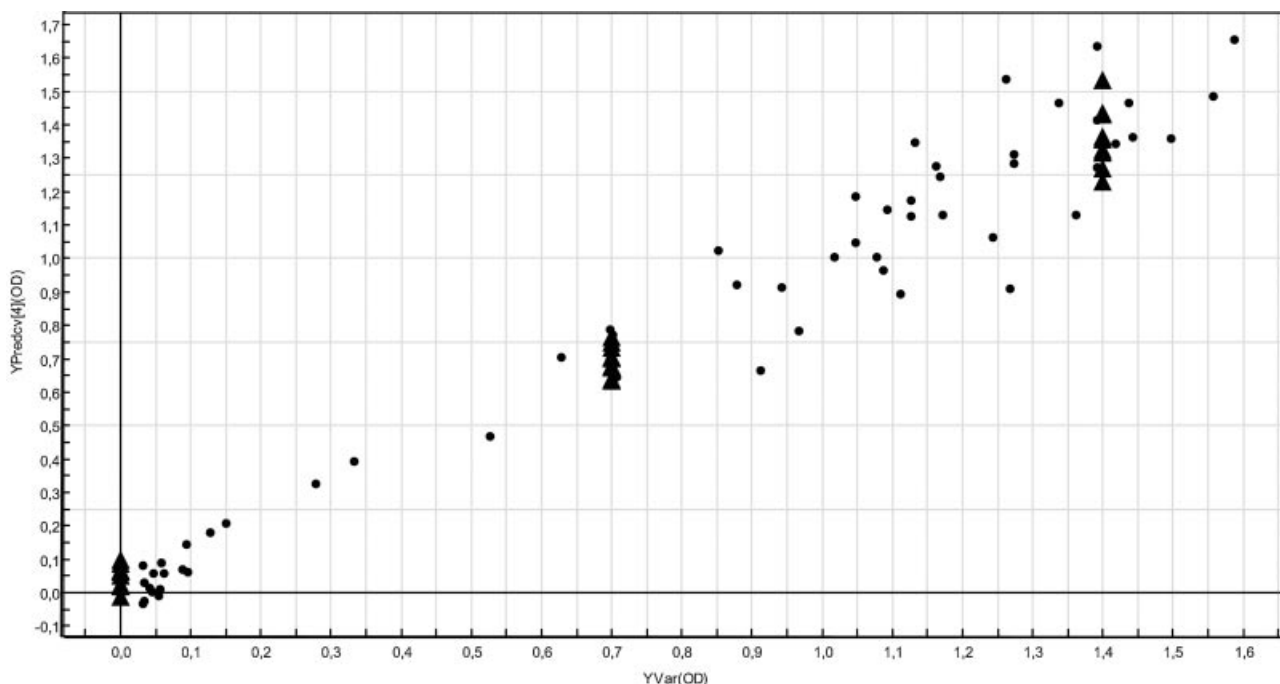


**Figure 4.** Plot showing values of  $OD_{590}$  predicted during cross-validation (ordinate) versus measured/prepared values (abscissa) of  $OD_{590}$ . Circles represent samples from original cultivation, while triangles represent artificial samples.

be used. The available data were sufficient to build a robust process model. In order to allow all datasets to be processed in a similar way, any gaps in the datasets were filled using averaged values in such a way that they did not influence the model.

### *Modeling of Dynamic Evolution*

Modeling of these kind of data can be performed according to several approaches. The most common approaches to model three-way data arrays are those by Nomikos and MacGregor (1994) and Wold et al. (1998, 2008). A discussion of approaches for batch data modeling can be found in Kourtogianni (2006) or Lopes et al. (2004). We have also discussed the approach for this specific dataset earlier (Van Sprang et al. 2007). The approach by Wold et al. (1998, 2008) is most suitable for this specific dataset, because of the nature of the dataset and the limited number of batches available. The process variables together with predicted OD<sub>590</sub> and NIR fingerprint variables were modeled using PLS with time as the Y variable. Prior to modeling, all variables were investigated individually and trimmed to remove unrepresentative values (e.g., spikes caused by air bubbles in the NIR measurement slit). The resulting PLS model based on all on-line signals from the bioreactor control system, the predicted biomass and the NIR fingerprint variables, describes the evolution of the cultivation batches as a result of the settings chosen in the DoE matrix (Table I). This is called a dynamic evolution model.

This model consists of two phases, each containing four components which explain >99% of process variance, as shown in Figures 5 and 6. The line graphs show the evolution of the loading plots for each batch over time, which the bars (loading plot) indicate the contribution of each parameter to the observed variance. A detailed interpretation of these components is provided in Appendix, while a short summary is given below. Note that it is not critical that all components be fully understood for a monitoring model. When, however, this model is used for the next level of modeling, the multivariate batch monitoring model, it is important that it encompasses “normal” batch evolution, in other words that it describes the process design space completely. It should thus distinguish normal or good batches from deviating batches. Because of the limited number of batches used in the experimental design, this will initially give ambiguous results in parts of the design space that are not fully covered in the experimentation. Data from new cultivations (for instance from regular manufacturing) should be added to the process model to make it more reliable over time. The model may also be challenged with experimental faulty batches for validation purposes.

The batch evolution was split into two phases coinciding with a switch in the oxygen control strategy (Figs. 5 and 6, respectively). At the start of a batch, before inoculation, dissolved oxygen (DO) is maintained at set-point using air

and N<sub>2</sub> with a total flow of 1 L/min. After inoculation, while maintaining a total flow of 1 L/min oxygen, consumption rises and the fraction of nitrogen decreases to zero. Simultaneously, the stirrer speed is gradually increased to a maximal set-point value. When both air and stirrer speed have reached their maximum set-points, the controller switches to a new strategy in which the fraction of oxygen in the gas mixture is increased by mixing pure O<sub>2</sub> into the airflow, while still maintaining total gas flow at 1 L/min. This relationship is seen in the first component for the first phase, where PredictedOD, air, stirring, and NIR\_fp1 are increasing with batch evolution while N<sub>2</sub> is decreasing.

The second phase of the process (Fig. 6) begins when the stirrer speed is no longer increasing and the pure oxygen valve is opened for the first time. This change in control strategy is clearly seen in the first component for the second phase, where PredictedOD and NIR\_fp1 continue to increase, while air decreases and O<sub>2</sub> increases. Further, more detailed, explanation of the model components is given in Appendix.

### *Multivariate Batch Monitoring Model*

For on-line monitoring whether any given process is running inside the process design space, a multivariate batch monitoring model is required. The batch monitoring model was constructed based on the dynamic evolution model as described in Wold et al. (2008). This model gives a total overview of the difference between the batches. To illustrate this, a PCA model with two components was built on the scores from the dynamic evolution model. The scores plot of this model is shown in Figure 7.

This plot is a 2D graphical representation of the process design space as it is described by the DoE batches. All batches are condensed into one point and the outer circle represents the 95% confidence interval of the (design) space defined by these points. The numbers correspond with the batch numbers shown in Table I. Batches 3 and 6B are not represented because of insufficient NIR and process data, as explained earlier.

All relevant process data, including the predicted OD and the NIR fingerprint variables, are condensed in the multivariate batch monitoring model. Figure 7 shows that the design applied can be seen to have caused some variation in the process evolution. The batches are similar—none fall outside of the Hotellings T<sub>2</sub> ellipse that represents a 95% confidence interval. The design is clearly reflected in the plot, as the center-points of the design (those batches run with intermediate values of all six investigated parameters), Batches 4, 5, 8, and 11, are close together and near the center of the graph. Furthermore a separation in temperature can be observed, with at the bottom and right part the cultures at 33°C (squares), in the middle the cultures run at 35°C (circles) and at the left and top part the cultures run at 37°C. Also a separation in the reactor used can be seen with the runs

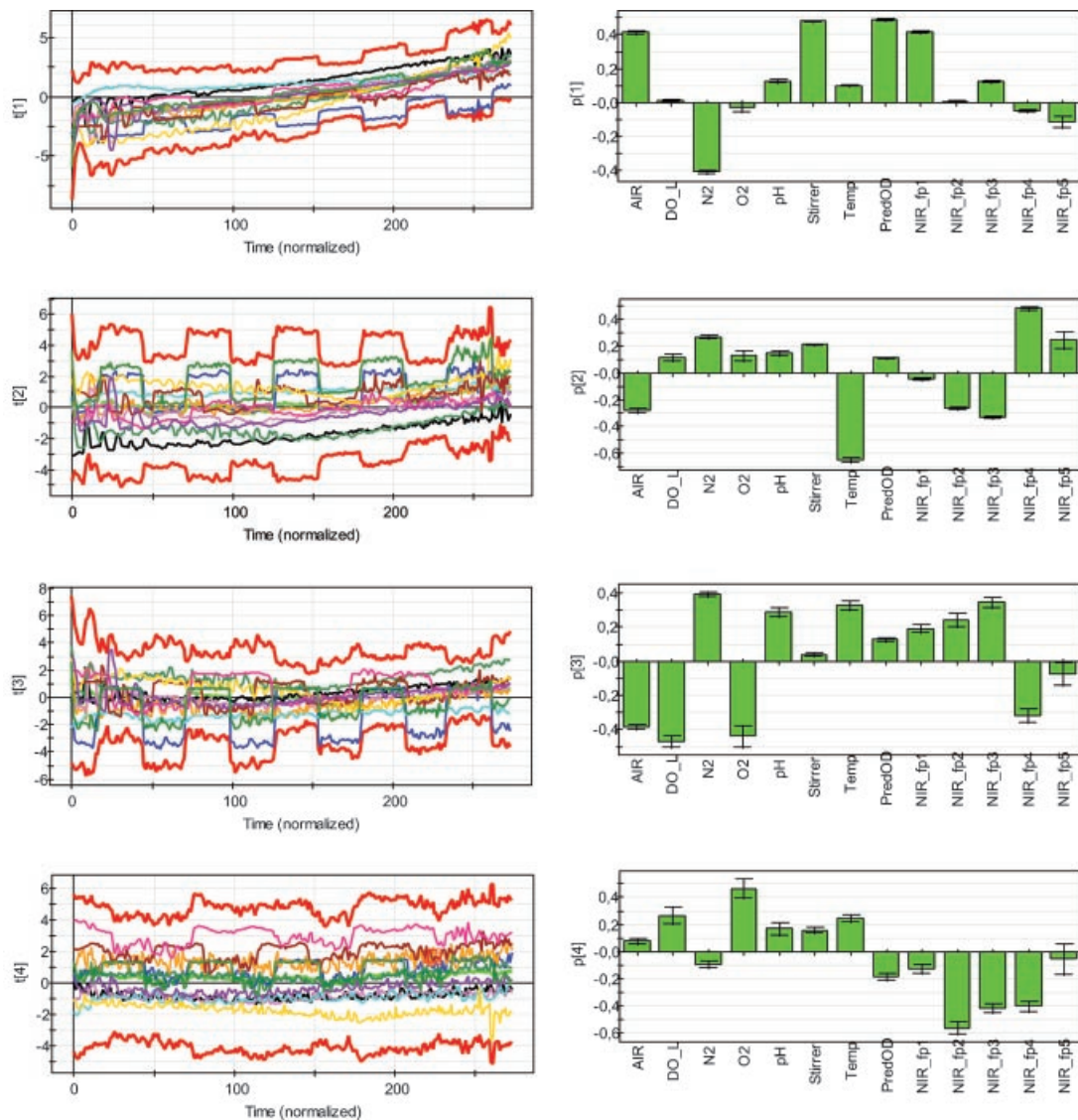


**Figure 5.** Scores (left) and loadings (right) of Phase 1 of components 1–4 (top to bottom) of the dynamic evolution model. The outer red lines in the line graphs indicate a 95% confidence interval and the green line the average. The other lines each represent the evolution of the score of a cultivation batch over time. The loadings (right) are represented as contribution plot in which the contribution of each individual parameter to the variance is shown. Error bars indicate the standard deviation over time. [Color figure can be seen in the online version of this article, available at [www.interscience.wiley.com](http://www.interscience.wiley.com).]

in reactor A (open symbols) being higher in the plot than the runs in Reactor B (closed symbols).

Because all batches were concluded to be of good quality, this plot—including the ellipse at the 95% confidence interval—can be viewed as a design space. However, the present dataset is insufficient to allow release decisions based on this model, because the present model does not fully describe the process design space. A batch with a combination of variables that is not tested in the DoE setup may fall outside the current design space, but still be of good quality or, on the other hand, may fall inside the design space and be of insufficient quality. As mentioned above, data from new batches must be added to the model to increase its accuracy, especially near the edges of the process design space.

## Conclusions

This report demonstrates how the general principles of PAT and design space can be applied to an undefined biopharmaceutical. The complexity of a bacterial cultivation process first requires sound scientific investigation of the critical process and product attributes and the analyses needed to measure these attributes. Mandatory QC assays may not provide the exact scientific information necessary to appraise product quality. A “pass” or “fail” result is usually insufficient in this case. The quality of the bacterial suspension at the end of cultivation was appraised using a product quality score derived from DNA microarray analysis. This provides a quantitative measure of the

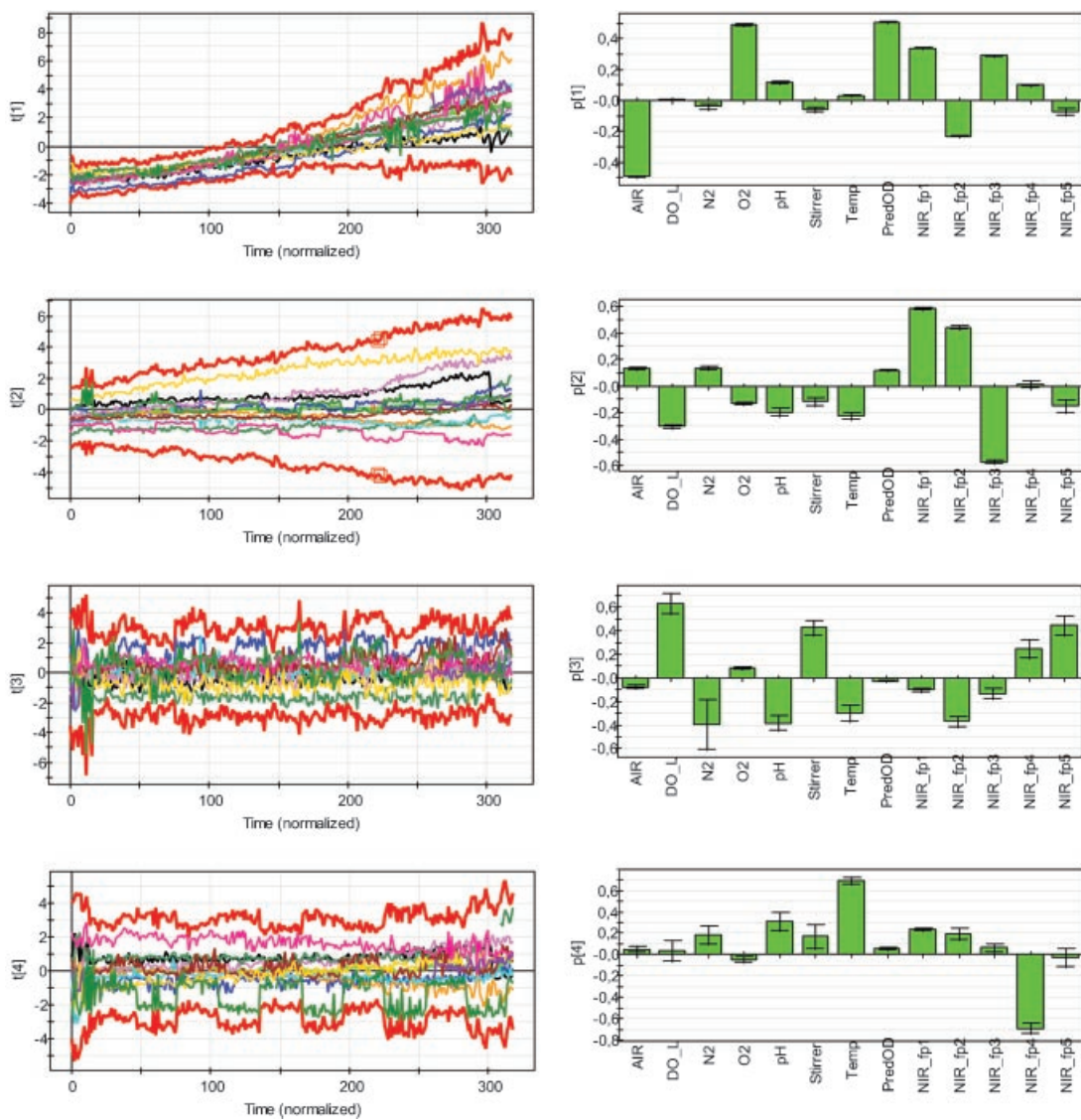


**Figure 6.** Scores (left) and Loadings (right) of Phase 2 of components 1–4 (top to bottom) of the dynamic evolution model. The outer red lines in the line graphs indicate a 95% confidence interval and the green line the average. The other lines each represent the evolution of the score of a cultivation batch over time. The loadings (right) are represented as contribution plot in which the contribution of each individual parameter to the variance is shown. Error bars indicate the standard deviation over time. [Color figure can be seen in the online version of this article, available at [www.interscience.wiley.com](http://www.interscience.wiley.com).]

performance of the run. The already available on line data were supplemented with NIR spectroscopy and samples were taken frequently to determine nutrient and biomass concentrations. This whole set of data contains all relevant information for this process step.

This report shows how this complex data set can be integrated into a single process model that describes the process design space for the cultivation of *B. pertussis* bacteria for the production of a whole cell vaccine against whooping cough disease. The steps that were undertaken for the development of this model are described; from experimental design and analytical (PAT) methodology to chemometrics and mathematics. The resulting model can be used to monitor process evolution on-line and make

predictions on the expected product quality at the end of cultivation.

Future application of this approach to all manufacturing process steps will allow the development of an overall manufacturing model incorporating the input and output of each process step, thus enabling flexible manufacturing at optimal settings. When this is validated, any process that has been executed within the process design space is assured to be of the specified quality. This means that this process model can make the release decision of the product during processing. Of course, to be allowed to replace mandatory QC testing, the model must be confirmed through extensive testing using actual process data. The model presented in this article may be considered a starting point for this

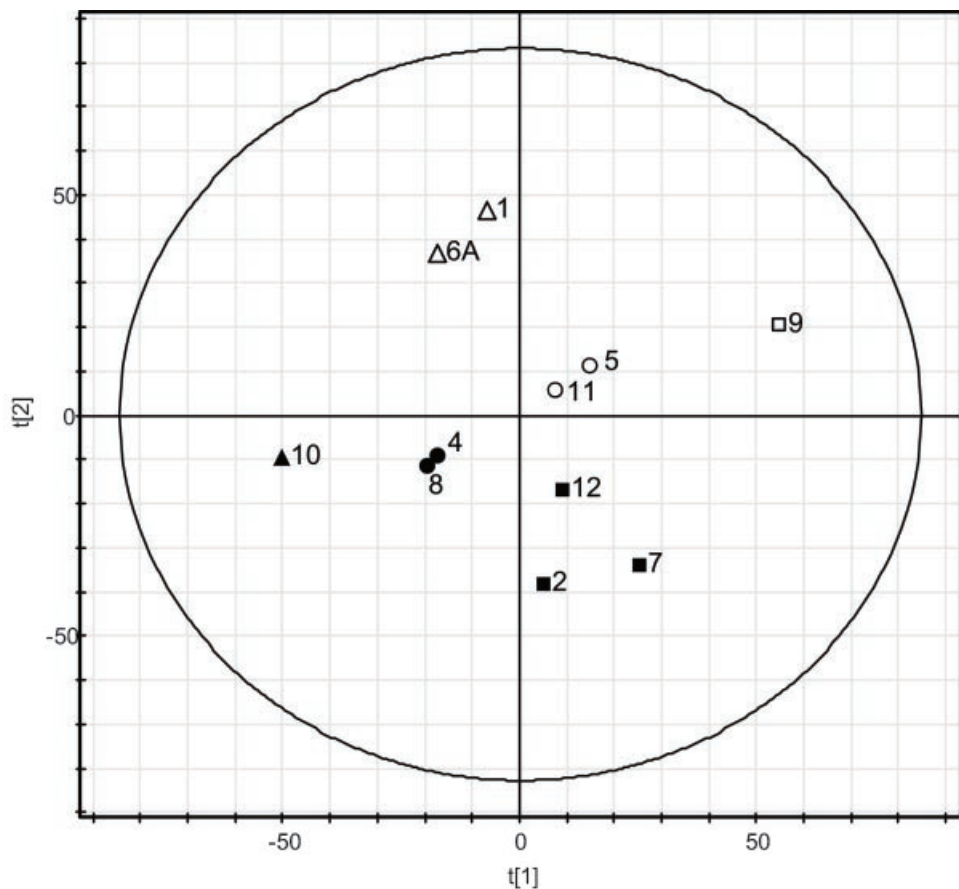


**Figure 7.** Overview of the multivariate batch monitoring model. Batches marked with triangles were run at 37°C, with circles at 35°C and with squares at 33°C. Open symbols represent the batches run in Reactor A and closed symbols batches run in Reactor B. The numbers denote the batch numbers as denoted in Table I.

procedure. It should be run in parallel to the normal testing procedures and, when sufficient data is added to the model and regular tests have confirmed its reliability and comparability, it can eventually replace these tests. The resulting system is then capable of... *analyzing, and controlling manufacturing through timely measurements (i.e., during processing) of critical quality and performance attributes of raw and in-process materials and processes with the goal of ensuring final product quality*, fulfilling the PAT definition.

## Appendix: Interpretation of the Model Components

### Phase 1

The first component represents a feature that increases throughout the batch evolution. It consists of a correlation between main variables air, stirring, PredictedOD and the first NIR fingerprint (NIR\_fp1), which is mainly the offset that also explains OD. These all increase while N<sub>2</sub> is decreasing. This is a logical correlation since they all follow general trends caused by bacterial growth during batch

cultivation. Increases in oxygen consumption cause the fraction air to increase over the fraction pure N<sub>2</sub>, and combine with an increasing stirrer speed and of course increased optical density.

The second component consists mainly of a correlation between temperature and NIR\_fp4. This is simply a confirmation that temperature is reflected in the NIR spectra.

The third component shows air, DO, and O<sub>2</sub>, together with NIR\_fp4 decreasing, while N<sub>2</sub>, pH, Temperature and NIR\_fp3 increase. This might just be an effect caused by the different DO setpoints in combination with temperatures in each batch. Although dissolved oxygen (DO) is stable throughout each batch, between batches there are differences between the N<sub>2</sub>/air ratios needed to maintain the setpoint. When the setpoint of DO is low, more nitrogen and less air is needed. This component also picks up an increase in pH that occurs mainly at the end of Phase 1. These phenomena may be caused by the fact that the oxygen transport constant between liquid and gas ( $k_{La}$ ) is dependent on temperature. At lower temperatures  $k_{La}$  is lower, which means a higher oxygen concentration in the gas phase is needed to maintain the setpoint. Also the solubility

of CO<sub>2</sub> (as H<sub>2</sub>CO<sub>3</sub>) is increased which results in a reduction in pH.

The fourth component shows that O<sub>2</sub> is negatively correlated with primarily NIR\_fp2. Close examination of the scores plot shows that this component reflects a difference between the reactors–batches run in Reactor A have low score values and batches run in Reactor B have high values. The variables NIR\_fp2 and NIR\_fp3 reflect some reactor difference (having higher values for Reactor A) and since the variable O<sub>2</sub> has a small variation between reactors—varying between 0 and 0.0005 for Reactor A but between 0 and 0.0015 for Reactor B, this component picks up a small negative correlation between the variable O<sub>2</sub> and the two NIR fingerprint variables.

## Phase 2

The first component, again, exhibits a rising trend for all batches. It consists mainly of a correlation between PredictedOD and increased NIR\_fp1, while air decreases and O<sub>2</sub> increases. This indicates an increased oxygen fraction in the gas flow due to the mixing of pure oxygen while reducing the air to maintain a constant gas flow. This phenomenon is accompanied by a strong increase in the optical density and it is reflected in the NIR\_fp1.

The second component shows a diverging pattern with some batches increasing while some decrease slightly. The correlation between the factors is relatively weak, except for the NIR fingerprints, where NIR\_fp1 and NIR\_fp2 strongly increase and NIR\_fp3 decreases. For the other factors, air, and N<sub>2</sub> and PredictedOD increase while all others (O<sub>2</sub>, pH, stirrer, temperature) decrease. This complex interaction cannot be readily explained but may be the result of several effects due to both bacterial growth and the *k<sub>L</sub>a* phenomenon described above.

The third component shows a rather noisy pattern, which is reflected by the larger error bars in the loading plot. Predominantly, an increase in DO and stirrer is accompanied by a decrease in N<sub>2</sub>, pH and temperature. The strong effect of pH is hard to explain, but the others are parameters that have been correlated earlier. This seems to be another difficult to explain, complex interaction but it may be due to the influence of several effects arising from the different set points for all experiments in the design.

The fourth component shows a slightly less noisy pattern than the third, but it is still largely unstructured. It mainly involves a correlation between pH and temperature. This can be explained by the aforementioned phenomenon that CO<sub>2</sub> (which is produced by the bacteria in the fermentor) dissolves better at low temperatures and, since it dissolves as a weak acid (H<sub>2</sub>CO<sub>3</sub>), reducing the pH.

## References

- Cummings CA, Bootsma HJ, Relman DA, Miller JF. 2006. Species- and strain-specific control of a complex, flexible regulon by *Bordetella* BvgAS. *J Bacteriol* 188(5):1775–1785.
- FDA. 2004. Guidance for Industry, PAT—A framework for innovative pharmaceutical development, manufacturing and quality assurance. <http://www.fda.gov/cder/guidance/6419fnl.pdf>.
- Harms J, Wang X, Kim T, Yang X, Rathore AS. 2008. Defining process design space for biotech products: Case study of *Pichia pastoris* fermentation. *Biotechnol Prog* 24(3):655–662.
- ICH. 2005. Pharmaceutical Development (Q8). International Conference on Harmonisation of Technical Requirements for Registration of Pharmaceuticals for Human Use <http://www.ich.org/LOB/media/MEDIA1707.pdf>.
- Irwin JO, Standfast AF. 1957. The intracerebral mouse-protection test for pertussis vaccines. *J Hyg (Lond)* 55(1):50–80.
- Kasahara T, Miyazaki T, Nitta H, Ono A, Miyagishima T, Nagao T, Urushidani T. 2006. Evaluation of methods for duration of preservation of RNA quality in rat liver used for transcriptome analysis. *J Toxicol Sci* 31(5):509–519.
- Kendrick PL, Eldering G, Dixon MK, Misner J. 1947. Mouse protection tests in the study of pertussis vaccine: A comparative series using the intracerebral route for challenge. *Am J Public Health Nations Health* 37(7):803–810.
- Kourti T. 2006. Process analytical technology beyond real-time analyzers: The role of multivariate analysis. *Crit Rev Anal Chem* 36(3–4):257–278.
- Lopes JA, Costa PF, Alves TP, Menezes JC. 2004. Chemometrics in bioprocess engineering: Process Analytical Technology (PAT) applications. *Chemometr Intell Lab Syst* 74(2):269–275.
- Montgomery DC. 2001. Experimental design for product and process design and development. *J R Statist Soc* 48(2):159–177.
- Mutter GL, Zahrieh D, Liu C, Neuberg D, Finkelstein D, Baker HE, Warrington JA. 2004. Comparison of frozen and RNALater solid tissue storage methods for use in RNA expression microarrays. *BMC Genomics* 5(1):88.
- Nomikos P, MacGregor JF. 1994. Monitoring batch processes using multiway principal component analysis. *AICHE J* 40(8):1361–1375.
- Ramalho AS, Beck S, Farinha CM, Clarke LA, Heda GD, Steiner B, Sanz J, Gallati S, Amaral MD, Harris A. 2004. Methods for RNA extraction, cDNA preparation and analysis of CFTR transcripts. *J Cyst Fibros* 3(Suppl 2):11–15.
- Streefland M, van de Waterbeemd B, Happe H, van der Pol LA, Beuvery EC, Tramper J, Martens DE. 2007. PAT for vaccines: The first stage of PAT implementation for development of a well-defined whole-cell vaccine against whooping cough disease. *Vaccine* 25(16):2994–3000.
- Streefland M, van de Waterbeemd B, Kint J, van der Pol LA, Beuvery EC, Tramper J, Martens DE. 2008. Evaluation of a critical process parameter: Oxygen limitation during cultivation has a fully reversible effect on gene expression of *Bordetella* pertussis. *Biotechnol Bioeng* 102(1):161–167.
- Thalen M, van den IJssel J, Jiskoot W, Zomer B, Roholl P, de Gooijer C, Beuvery C, Tramper J. 1999. Rational medium design for *Bordetella* pertussis: Basic metabolism. *J Biotechnol* 75(2–3):147–159.
- Van de Waterbeemd B, Streefland M, Pennings J, Van der Pol L, Beuvery C, Tramper J, Martens D. 2009. Gene-expression based quality scores indicate optimal harvest point in bacterial vaccine production. *Biotechnol Bioeng* 103(5):900–908.
- Van Sprang ENM, Streefland M, Van der Pol LA, Beuvery EC, Ramaker HJ, Smilde AK. 2007. Manufacturing vaccines: An illustration of using PAT tools for controlling the cultivation of *Bordetella pertussis*. *Qual Eng* 19(4):373–384.
- Wold S, Kettaneh N, Friden H, Homberg A. 1998. Modelling and diagnostics of batch processes and analogous kinetic experiments. *Chemometr Intell Lab Syst* 44(1–2):331–340.
- Wold S, Kettaneh N, MacGregor J, Dunn K. 2008. Batch processes: Modelling, analysis and control. In: Walczak B, Tauler Ferré R, Brown S, editors. *Comprehensive chemometrics*. Amsterdam, The Netherlands: Elsevier.
- Xing D, Das RG, O'Neill T, Corbel M, Dellepiane N, Milstien J. 2001. Laboratory testing of whole cell pertussis vaccine: A WHO proficiency study using the Kendrick test. *Vaccine* 20(3–4):342–351.